

Target Detection for Marine Radars Using a Data Matrix Bank Filter

Moon Kwang Jang* · Choon Sik Cho

Abstract

Marine radars are affected by sea and rain clutters, which can make target discrimination difficult. The clutter standard deviation and improvement factor are applied using multiple parameters—moving speed of radar, antenna speed, angle, etc. When a radar signal is processed, a Data Matrix Bank (DMB) filter can be applied to remove sea clutters. This filter allows detection of a target, and since it is not affected by changes in adjacent clutters resulting from a multi-target signal, sea state clutters can be removed. In this paper, we study the level for clutter removal and the method for target detection. In addition, we design a signal processing algorithm for marine radars, analyze the performance of the DMB filter algorithm, and provide a DMB filter algorithm design. We also perform a DMB filter algorithm analysis and simulation, and then apply this to the DMB filter and cell-average constant false alarm rate design to show comparative results.

Key Words: Cell-Average Constant False Alarm Rate, Clutter Standard Deviation, Data Matrix Bank Filter, Improvement Factor, Marine Radar, Rain Clutter, Sea Clutter.

I. Introduction

Marine radars with an S-band of 3 GHz and X-band of 10 GHz are currently used worldwide. However, marine radars are significantly affected by sea and rain clutters, so difficulties emerge when attempting to discriminate targets from the clutters. Therefore, precise detection technology is needed for target classification; in other words, marine radars need to correctly distinguish between targets and clutters. A number of methods are currently available to do this; for example, marine radars can remove low frequency clutters by applying Gaussian distribution in the marine radar environment. Nevertheless, improvements in marine radar target detection capabilities are still needed to tackle the high clutter region, but successfully overcoming marine radar signal processing problems requires, high computing capacity and large amount of memory.

The cell-average constant false alarm rate (CA-CFAR) algorithm continuously calculates the average value based on previously measured values. However, the CA-CFAR is inefficient in the case of small size targets and non-moving Doppler. And it also experiences difficulties in target detection with high frequency clutters. The CA-CFAR is also inefficient in cases where large changes in noise occur. In this paper, we propose a Data Matrix Bank (DMB)

filter algorithm for improving target detection and clutter removal. The wave height of the sea state can be represented by the size of the standard used to measure wave height, as shown in Table 1. The sea states shown in Table 1 are used by the World Meteorological Organization. Sea state can be classified depending on the Douglas scale, Hydrographic Office scale, and Beaufort scale. Wind speed is affected by the clutter size. The distance depends on how far and how fast the wind blows, how it advan-

Table 1. Sea states used by the World Meteorological Organization [2]

Sea state	State name	Wave height(m)
0	Not recognized	0
1	Smooth	0 – 0.1
2	Slight	0.1 – 0.5
3	Moderate	0.6 – 1.2
4	Rough	1.2 – 2.4
5	Very rough	2.4 – 4.0
6	High	4.0 – 6.0
7	Very high	6.0 – 9.0
8	Precipitous	9.0 – 14.0

Manuscript received January 30, 2013 ; Revised June 5, 2013 ; Accepted June 10, 2013. (ID No. 20130130-005J)

Department of Telecommunication & Information Engineering, Korea Aerospace University, Goyang, Korea.

*Corresponding Author : Moon Kwang Jang (e-mail : mkjang@kau.ac.kr)

This is an Open-Access article distributed under the terms of the Creative Commons Attribution Non-Commercial License (<http://creativecommons.org/licenses/by-nc/3.0>) which permits unrestricted non-commercial use, distribution, and reproduction in any medium, provided the original work is properly cited.

Table 2. Clutter standard deviation (SD) of sea clutter [3]

Sea state	State name	Clutter SD
0	Not recognized	None
1	Smooth	0–25
2	Slight	25–75
3	Moderate	75–120
4	Rough	120–190
5	Very rough	190–250
6	High	250–370
7	Very high	370–600
8	Precipitous	>600

ces, and the impact has [1].

Table 2 represents the clutter spectrum hitting the surface of sea, which reflects the standard deviation of the clutter spectrum. The CFAR algorithm has a fixed threshold that determines this simply by considering only the noise level of the surrounding clutters. The CFAR can have a variable adaptive threshold depending on the environment. The adaptive threshold CFAR is representative of the CA-CFAR; and the order statistics constant false alarm rate (OS-CFAR). The CA-CFAR consumes a lot of memory because it works by calculating around the average. Detection performance is greatly lowered because it may occur, for example, in situations such as when an adjacent interference target is present with multiple targets. Clutter removal performance will be degraded in accordance with changes that depend on the target size signal and noise. Here, a DMB filter is proposed to resolve these problems.

We added a comparator and database in Fig. 2 to allow a more systematic decision of the real targets. The database, consisting of improvement factors and standard deviations for sea and rain clutters, was established using verified results referred from [2-5]. Tables 1–5 show these data that clarify the clutters used in this work. The amplitudes of targets become larger than those of the clutters presented in our previous work [6] due to the more accurate algorithm used in the present work. Therefore, any targets can be detected more accurately using the improved DMB algorithm which therefore represents an enhancement of our previous work [6].

II. Clutter Analysis

The improvement factor and the clutter standard deviation can be obtained using the return frequency from sea. The Doppler frequency changes the clutter standard deviation along with the moving speed of the radar, antenna speed, angle, etc. The IEEE definition of an improvement

factor (I) reads: the signal-to-clutter power ratio at the output of the clutter filter divided by the signal-to-clutter power ratio at the input to the clutter filter, averaged uniformly over all target radial velocities of interest. The improvement factor can be expressed as in Eq. (1) [7].

$$I = \frac{(S/C)_{out}}{(S/C)_{in}} \tag{1}$$

where S is the signal and C is the clutter. The clutter standard deviation (σ_v) of the Gaussian clutter spectrum can be defined as in Eq. (2) [3].

$$\sigma_v = aW_s^b \tag{2}$$

where σ_v is the clutter standard deviation, W_s is the wind speed, a is 0.101 for Sea clutters and 0.0045 for woodlands, and b is 0.36 for sea clutters and 1.4 for woodlands. Clutter Doppler frequency changes depending on the moving speed of the radar and change in the vertical and horizontal angle of the antenna beam, but removal of the clutter is easier using the clutter standard deviation method than with any other method. Marine radars can classify targets by interpreting clutter spectrum changes using the clutter standard deviation in the x axis and the improvement factor in the y axis. In this paper, the data in Tables 3–5, as shown in Fig. 1, are applied to the matrix Table [8]. Tables 3–5 show the values of the $M(i, j)$ used to detect clutter in the DMB filter clutter map for the sea and rain at the control level [6]. Az is the azimuth of the horizontal angle of the antenna beam angle and Dep is the depression of the vertical antenna beam angle.

Table 3. Basic modes [4, 5]

Wind speed (knot)	Clutter	Az	Dep	Improvement factor	SD
10	Sea	0	30	52.9	31.8
10	Sea	0	80	51.6	31.8
10	Sea	30	30	52.6	33.0
10	Sea	30	80	35.6	86.0
10	Rain	0	30	41.3	50.0
10	Rain	0	80	42.2	50.0
10	Rain	30	30	46.6	52.0
10	Rain	30	80	38.8	93.0
30	Sea	0	30	34.3	95.6
30	Sea	0	80	34.8	95.6
30	Sea	30	30	37.1	96.0
30	Sea	30	80	34.4	124.0

Az=the azimuth of the horizontal antenna beam's angle, Dep=the depression of the vertical antenna beam's angle, SD=standard deviation.

Table 4. Low speed modes [4, 5]

Wind speed (knot)	Clutter	Az	Dep	Improvement factor	SD
10	Sea	0	30	54.4	32.0
10	Sea	0	80	51.4	32.0
10	Sea	30	30	48.5	32.0
10	Sea	30	80	41.2	65.0
10	Rain	0	30	42.6	50.0
10	Rain	0	80	47.5	50.0
10	Rain	30	30	50.8	50.0
10	Rain	30	80	38.9	75.0
30	Sea	0	30	34.7	95.6
30	Sea	0	80	37.6	95.6
30	Sea	30	30	39.4	95.6
30	Sea	30	80	33.7	111.0

Az=the azimuth of the horizontal angle of the antenna beam angle, Dep=the depression of the vertical antenna beam angle, SD=standard deviation.

Table 5. High speed modes [4, 5]

Wind speed (knot)	Clutter	Az	Dep	Improvement factor	SD
10	Sea	0	30	46.37	31.88
10	Sea	0	80	56.12	31.88
10	Sea	30	30	52.58	32.04
10	Sea	30	80	34.51	128.45
10	Rain	0	30	46.25	50.00
10	Rain	0	80	42.11	50.00
10	Rain	30	30	41.64	50.11
10	Rain	30	80	30.48	134.10
30	Sea	0	30	37.35	95.60
30	Sea	0	80	34.36	95.60
30	Sea	30	30	34.45	95.60
30	Sea	30	80	28.70	156.93

Az=the azimuth of the horizontal angle of the antenna beam angle, Dep=the depression of the vertical antenna beam angle, SD=standard deviation.

Marine radars generally have basic, low speed, and high speed modes. Tables 3–5 show that the low speed mode has a small clutter standard deviation, but the high speed mode has an increasing clutter standard deviation, while the size of improvement factor is constant [8, 9]. When the angle of antenna (depression) is 30°, the clutter standard deviation is kept almost constant. When the angle of the antenna (depression) is increased to 80°, the clutter standard deviation somewhat increases by about

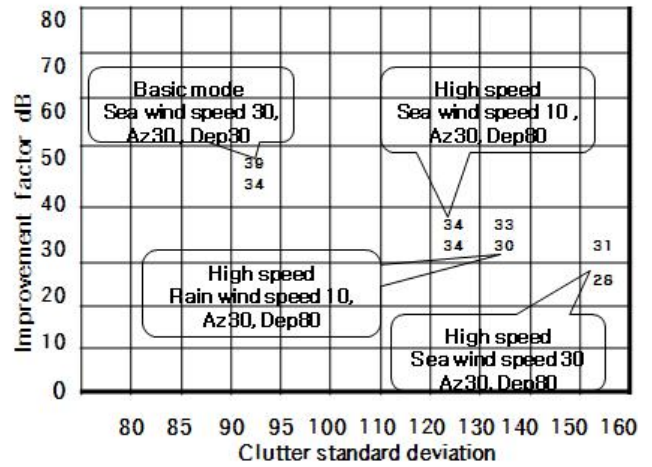


Fig. 1. Matrix using improvement factors (I) and clutter standard deviation (σ_v).

30 to 40.

III. DMB Filter

The DMB filter, a new target detection technology, is proposed for this study. It uses an $I - \sigma_v$ matrix that works by reacting to changes in standard deviation. This enables the detection of a target using the improvement factor and the clutter standard deviation in the spectrum.

1. Block Diagram

A DMB filter block diagram is shown in Fig. 2. The DMB filter uses the improvement factors and clutter standard deviations both from measured data and pre-calculated data base as in Table 6. The DMB filter is configured to compare $H(i, j)$ to $M(i, j)$ in a database composed of the improvement factor (I) and clutter standard deviation (σ_v).

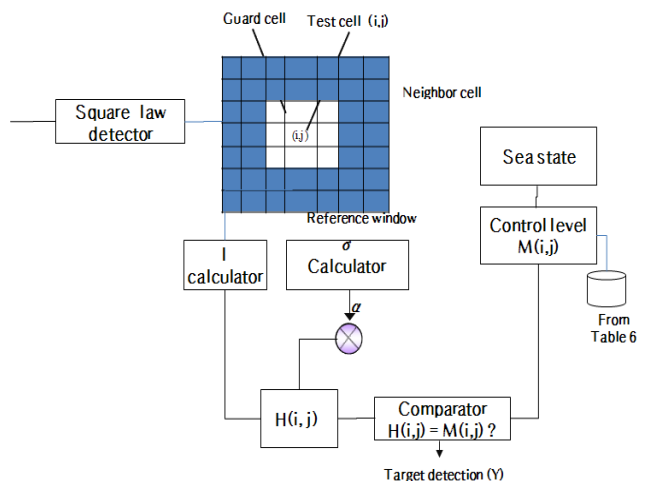


Fig. 2. A block diagram of data matrix bank filter.

Table 6. Values for the DMB MAP database (sea) [4]

Key	Wind speed* (knot)	Az*	Dep*	Improve-ment factor*	SD*	Level (sea state)	Remark
1	10	0	30	52.90	31.88	5	Basic sea
2	10	0	80	51.67	31.88	5	Basic sea
3	10	30	30	52.64	31.94	5	Basic sea
4	10	30	80	35.69	85.36	8	Basic sea
5	30	0	30	34.36	95.63	9	Basic sea
6	30	0	80	34.82	95.63	9	Basic sea
7	30	30	30	37.12	95.65	9	Basic sea
8	30	30	80	34.44	124.15	9	Basic sea
9	10	0	30	41.36	50.00	6	Basic rain
10	10	0	80	42.20	50.00	6	Basic rain
11	10	30	30	46.65	50.04	6	Basic rain
12	10	30	80	38.82	93.65	9	Basic rain

The asterisk (*) referred from Tables 3–5. DMB=Data Matrix Bank, Az=the azimuth of the horizontal angle of the antenna beam angle, Dep=the depression of the vertical antenna beam angle, SD=standard deviation.

The data indicated with * in Table 6 are brought from Tables 3–5 showing sea and rain clutters. These data are used for comparison with results using the DMB method proposed in this work. The key no. 1 to 7 are measures of sea clutters. The key no. 8 to 12 are measures of rain clutters. The level (=sea state) is classified using standard deviation as seen in Table 2 (the key value for the properties of the clutter stored attribute value is used to verify the data for one record or one unit clutter. A single record or a data retrieval clutter is one of the means used to verify the primary key).

1.1 Reference Window

The reference window in Fig. 2 shows a two-dimensional data vector of a range of cells measured at a specific time. The guard cell is data located next to the test cell. The neighbor cells are data located next to the guard cell, indicated in grey in Fig. 2.

1.2 Improvement Factor (I) and Clutter Standard Deviation (σ_v) Calculator

Eq. (3) shows $H(i, j)$ composed of the improvement factor and clutter standard deviation estimating equations about output (i, j) .

$$H(i, j) = I(i, j) + \alpha \sigma(i, j) \tag{3}$$

Where $H(i, j)$ is the DMB value measured at (i, j) , $I(i,$

$j)$ is the improvement factor, $\sigma_v(i, j)$ is the estimated clutter standard deviation, and α is the constant value used to decide the target.

1.3 Sea State

The user selects the target for detection. The user should select the type of clutter to get rid of the radar clutters.

1.4 Control Level

The control level is determined by the target value for improvement factor and clutter standard deviation by the user. The antenna speed, the speed of radar, the moving speed of radar, the speed of wind, the antenna azimuth angle, and the depression angle are also used for deciding this level.

1.5 Comparator

The control level is compared with $H(i, j)$ to decide whether the detection level is greater than the $M(i, j)$.

2. Performance Analysis

The probabilities of detection and false alarm are calculated to indicate how to obtain the correct values from the following procedures. The probability of detection (expected value of P_D) is expressed in Eq. (4) [10].

$$P_D = \exp\left(\frac{-M(i, j)}{1 + n_p SNR / 2}\right) \left(1 + \frac{2}{n_p SNR}\right)^{n_p - 2} \times K_0 \tag{4}$$

where

$$K_0 = 1 + \frac{M(i, j)}{1 + n_p SNR / 2} - \frac{2}{n_p SNR} (N_p - 2) \tag{5}$$

Where n_p is number of integrated pulses, signal-to-noise ratio is signal to noise ratio, and $M(i, j)$ is threshold value. The probability of detection from the DMB filter is shown in Fig. 3. The probability density function of Swerling III is detected once the proposed method is applied. The cell window is estimated for the 1-, 10-, 50-, and 100-cell cases. The probability of detection for each window appears as the number of cells to changes in the index of each cell by calculating the improvement factor and the clutter standard deviation, as shown in Fig. 3 [11]. A detection probability of over 0.90 is estimated to be the number of pulses, as shown in Fig. 3. This should be more than 10 cells. In Fig. 4, the DMB filter shows a CFAR of change in the number of pulses for the loss.

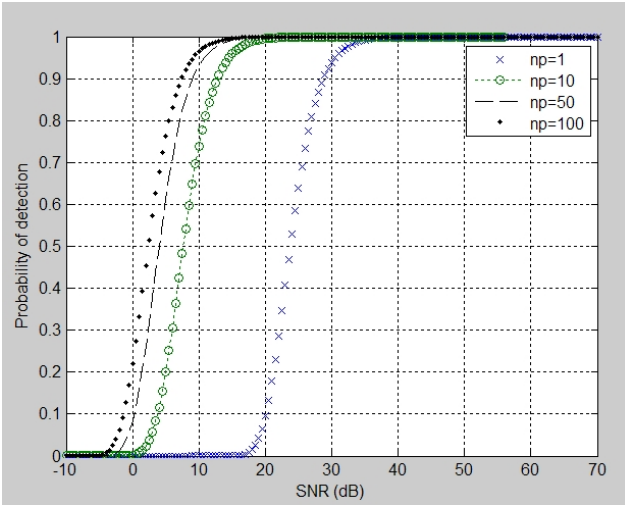


Fig. 3. Swerling III target (probability of detection=0.90). n_p =number of cells, SNR=signal-to-noise ratio.

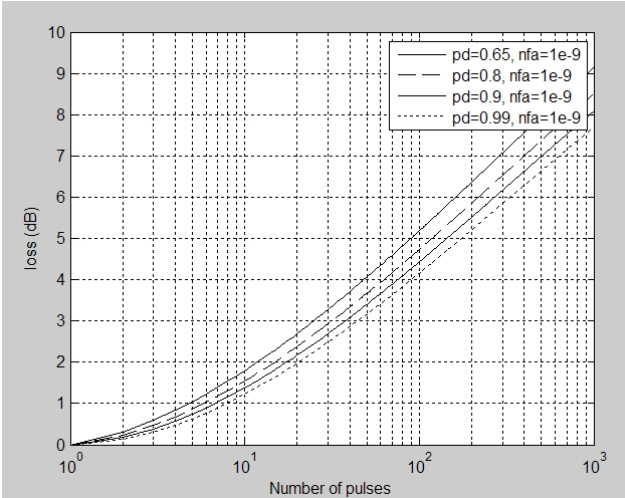


Fig. 4. Loss rate according to number of pulses. pd=probability of detection, nfa=Marcum's false alarm number).

IV. Simulation Results

Radar specifications are applied in order to validate the approach proposed in this paper as shown in Table 7, with the performance of the semiconductor solid state power amplifier radar. The radar specifications in Table 7 are decided by following the procedures in applying synthetic targets and a clutter matched filter.

First, a conventional CFAR target detection is used for comparison in Fig. 5. Target detection is used to calculate $H(i, j)$. $M(i, j)$ is used to retrieve the pre-calculated improvement factor and clutter standard deviation to compare the target that is greater than the value of the threshold. As indicated in Fig. 5, since the matched filter is connected to two processes, values from CFAR were

Table 7. Design specifics of the proposed radar

Specification	Design value
Sample frequency (MHz)	80
Pulse duration (μ sec)	3.3
Pulse repetition frequency (kHz)	3
Dwell time (μ sec)	16
Bandwidth (MHz)	30
Signal-to-noise ratio (dB)	30
Doppler frequency (MHz)	2
Probability of false alarm (P_{FA})	1×10^{-9}

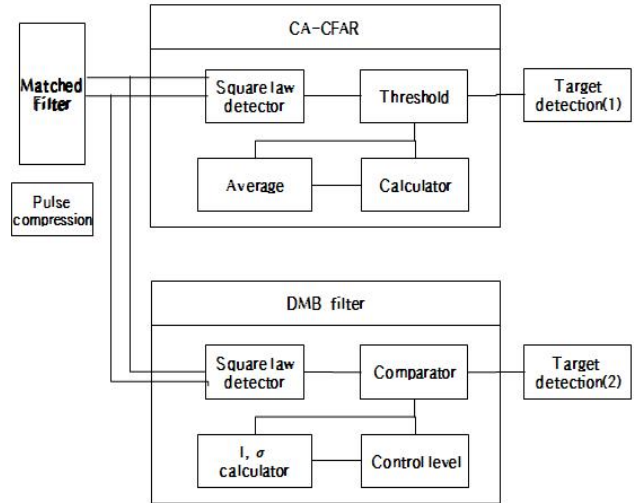


Fig. 5. Cell-average constant false alarm rate (CA-CFAR) and Data Matrix Bank (DMB) filter processes.

measured by applying the CA-CFAR, and the others are carried out by the matched filter using the DMB filter algorithm.

The target detection in CA-CFAR is weak as shown in Fig. 6, which shows that detection is very difficult because of the adjacent targets. The average of magnitude of the surrounding cells is lower than the threshold, as illustrated in Fig. 6. Fig. 7 enlarges the target surroundings based on CA-CFAR, where all targets are below the threshold.

Fig. 8 shows simulation results based on the proposed DMB filter. The DMB filter makes target detection possible, as shown in Fig. 8. Fig. 9 also shows target surroundings for the DMB filter, which makes the targets detectable since the targets are above the threshold.

Fig. 8 shows the performance of the proposed DMB filter. In order to remove any clutter from moving targets, we have to store the data in a standard DMB filter database. The improvement factor and clutter standard deviation are calculated, and used to perform clutter removal and target detection. Target detection is easy in a high sea

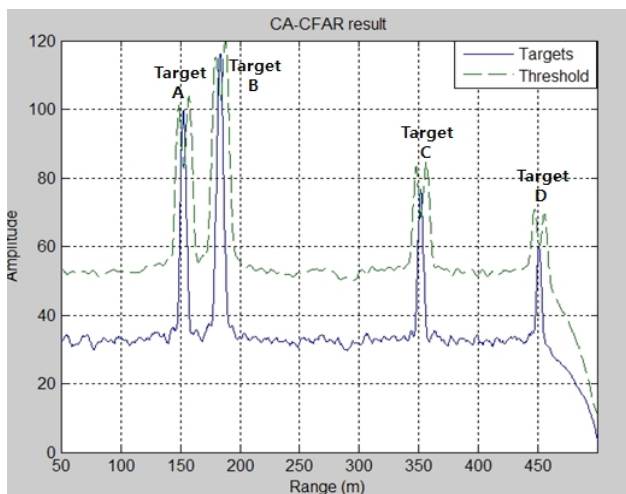


Fig. 6. Conventional cell-average constant false alarm rate (CA-CFAR) target detection.

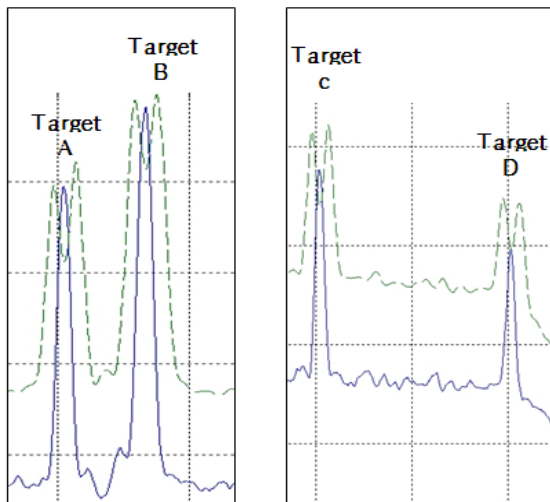


Fig. 7. Enlargement of targets A to D in Fig. 6.

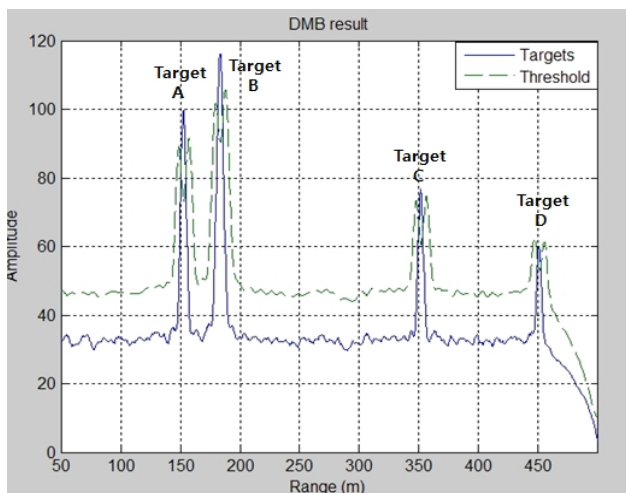


Fig. 8. Target detection of the proposed Data Matrix Bank (DMB) filter.

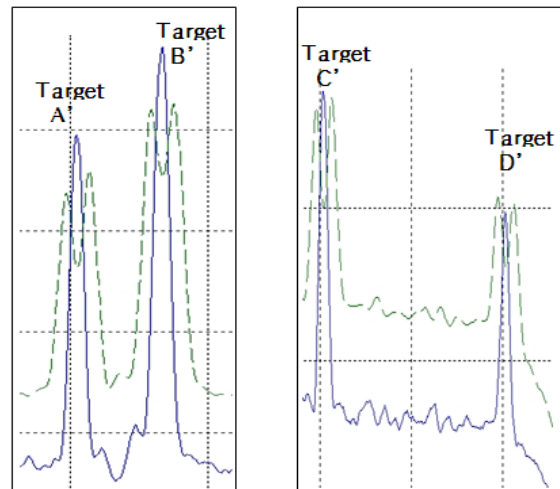


Fig. 9. Enlargement of targets A' to D' in Fig. 8.

level and high-frequency components of clutter can be detected at the same time. This method does not consume much memory, and can detect a target using the clutter signal. The probability of detection and loss rate for this DMB filter are shown in Figs. 3 and 4. The DMB filter works well in removing the effects interference signals of adjacent cells from multiple environments, as shown in Fig. 8.

V. Conclusion

Sea waves and rain are studied in order to remove clutter and to determine better methods for target detection. The DMB filter is unaffected by multi-target signal changes in the adjacent signal. Detection is accurate, as shown by mathematical theory and through a simulation. Marine radar performance ensures a highly capable DMB filter algorithm for signal processing, algorithm design, and simulation. The designed radar specifications using the DMB filter and CA-CFAR algorithm are applied to compare the performance indicators. A significantly improved performance is observed over CA-CFAR target detection when applying the proposed DMB filter.

References

- [1] F. E. Nathanson, M. N. Cohen, and J. P. Reilly, *Radar Design Principles: Signal Processing and the Environment*, 2nd ed., New York, NY: McGraw-Hill, 1991.
- [2] M. I. Skolnik, *Introduction to RADAR System*, 3rd ed. New York, NY: McGraw-Hill, 2001.
- [3] B. Edde, *RADAR Principles, Technology, Applications*. Englewood Cliffs, NJ: Prentice-Hall, 1993.
- [4] J. H. Bae, "Airborne Radar system design and Doppler target detection," M.S. thesis, School of Electronics

- Engineering, Korea Aerospace University, Goyang, Korea, 2005.
- [5] Y. K. Kwak, M. S. Choi, J. H. Bae, I. P. Jeon, K. Y. Hwang, J. Y. Yang, D. H. Kim, and J. W. Kang, "X-band pulsed Doppler radar development for helicopter," *Journal of the Korean Institute of Electromagnetic Engineering and Science*, vol. 17, no. 8, pp. 773-787, 2006.
- [6] M. K. Jang and C. S. Cho, "Target detection of marine radars using Matrix Bank filters," in *Proceedings of the 2012 Asia Pacific Microwave Conference*, Kaohsiung, China, 2012, pp. 1046-1048.
- [7] D. C. Schleher, *MTI and Pulsed Doppler Radar with MATLAB*, 2nd ed., Boston, MA: Artech House, 2010.
- [8] M. K. Jang and C. S. Cho, "Control about sea clutter level of marine radar," in *Proceedings of the 3rd International Asia-Pacific Conference on Synthetic Aperture Radar*, Seoul, Korea, 2011.
- [9] M. I. Skolnik, *Radar Handbook*, 2nd ed., New York, NY: McGraw-Hill, 1990.
- [10] B. R. Mahafza, *Radar Systems Analysis and Design Using MATLAB*, 2nd ed., Boca Raton, FL: Chapman & Hall/CRC, 2005.
- [11] M. A. Richards, *Fundamentals of Radar Signal Processing*. New York, NY: McGraw-Hill, 2005.

Moon Kwang Jang



received his B.S. in Computer Engineering from Inha University in 1988, his M.S. in Telecommunications and Computer Engineering from Korea Aerospace University in 2009. He is currently studying a Ph.D. course in the Department of Telecommunication & Information Engineering, Korea Aerospace University. He was with SAEDONG Engineering Inc., working in telecommunications and computer engineering field. His research interests include radar signal processing, software engineering, software certification, high efficiency active circuits, computational electromagnetics, and microwave and millimeter wave components design.

Choon Sik Cho



received his B.S. in Control and Instrumentation Engineering from Seoul National University in 1987, his M.S. in Electrical and Computer Engineering from the University of South Carolina in 1995, and his Ph.D. in Electrical and Computer Engineering from the University of Colorado in 1998. From 1987 to 1993, he was with LG Electronics, working on communication systems. From 1999 to 2003, he was with Curitel, where he was principally involved with the development of mobile phones. He joined the School of Electronics, Telecommunication and Computer Engineering at Korea Aerospace University in 2004. His research interests include the design of RFIC/MMIC, millimeter-wave ICs, analog circuits, imaging radars as well as wireless power transfer.